THE JOURNAL OF BIOLOGICAL CHEMISTRY Vol. 278, No. 31, Issue of August 1, pp. 29261–29266, 2003
Printed in U.S.A.

Calcium Dependence of the Interaction between Calmodulin and Anthrax Edema Factor*[S]

Received for publication, March 20, 2003, and in revised form, April 25, 2003
Published, JBC Papers in Press, April 29, 2003, DOI 10.1074/jbc.M302837200

Tobias S. Ulmer‡§, Sandriyana Soelaiman¶, Shipeng Li‖, Claude B. Klee‖, Wei-Jen Tang¶‡‡, and Ad Bax‡§§**

From the ‡Laboratory of Chemical Physics, NIDDK, and the ‖Laboratory of Biochemistry, NCI, National Institutes of Health, Bethesda, Maryland 20892 and the ¶Ben-May Institute for Cancer Research, University of Chicago, Chicago, Illinois 60637

Edema factor (EF), a toxin from *Bacillus anthracis* (anthrax), possesses adenylyl cyclase activity and requires the ubiquitous Ca^{2+}-sensor calmodulin (CaM) for activity. CaM can exist in three major structural states: an apo state with no Ca^{2+} bound, a two Ca^{2+} state with its C-terminal domain Ca^{2+}-loaded, and a four Ca^{2+} state in which the lower Ca^{2+} affinity N-terminal domain is also ligated. Here, the interaction of EF with the three Ca^{2+} states of CaM has been examined by NMR spectroscopy and changes in the Ca^{2+} affinity of CaM in the presence of EF have been determined by flow dialysis. Backbone chemical shift perturbations of CaM show that EF interacts weakly with the N-terminal domain of apoCaM. The C-terminal CaM domain only engages in the interaction upon Ca^{2+} ligation, rendering the overall interaction much tighter. In the presence of EF, the C-terminal domain binds Ca^{2+} with higher affinity, but loses binding cooperativity, whereas the N-terminal domain exhibits strongly reduced Ca^{2+} affinity. As judged by chemical shift differences, the N-terminal CaM domain remains bound to EF upon subsequent Ca^{2+} ligation. This Ca^{2+} dependence of the EF-CaM interaction differs from that observed for most other CaM targets, which normally interact only with the Ca^{2+}-bound CaM domains and become active following the transition to the four Ca^{2+} state.

Edema factor (EF)[1] is a calmodulin (CaM)-dependent adenylyl cyclase that is secreted by *Bacillus anthrax* (anthrax) to elevate cellular cAMP levels in host cells (1). Together with the proteins "protective antigen" and "lethal factor" it constitutes "anthrax toxin," the dominant virulence factor of anthrax (2). Lethal factor is a zinc metalloprotease, which cleaves and inactivates mitogen-activated protein kinase kinase (3). Protective antigen binds to a recently identified cell-surface receptor (4) and carries lethal and edema factor into the cell by receptor-mediated endocytosis.

CaM, a calcium sensor and signal transducer, is comprised of an N- and C-terminal domain, which each contain two Ca^{2+}-binding, helix-loop-helix motifs (5, 6). CaM can exist in three major structural states: an apo state with no Ca^{2+}-bound, a two Ca^{2+} state with its C-terminal domain mainly Ca^{2+}-loaded and its N-terminal domain mainly apo, and a four Ca^{2+} state in which the lower Ca^{2+} affinity N-terminal domain is also ligated. Upon Ca^{2+} binding the CaM domains switch from a "closed" conformation, with the two helices of each Ca^{2+}-binding, helix-loop-helix motif almost anti-parallel, to an "open" conformation, with the two helices nearly perpendicular (5, 6). These conformational rearrangements lead to the exposure of a number of hydrophobic residues and render apo- and Ca^{2+}-loaded CaM structurally quite distinct (5, 6). Most of the target enzymes of CaM utilize those exposed hydrophobic residues as interaction sites (7). The CaM-Ca^{2+} dissociation constants extend over the range of 10^{-6} to 10^{-5} M under physiological salt concentrations (8, 9). In resting cells, which contain about 0.05–0.1 μM free Ca^{2+} (10, 11), the apo state of CaM dominates. The release of Ca^{2+} from intracellular stores, or the gated Ca^{2+} influx from outside the cells, increases the concentration of free Ca^{2+} up to 1–2 μM (10, 11) and, consequently, increases the proportion of the Ca^{2+}-loaded states of CaM. Most physiological targets regulated by CaM interact only with the Ca^{2+}-bound domains and require the transition of CaM to the four Ca^{2+} state for activation (12). The selective binding and concomitant stabilization of the open domain states of CaM generally results in an increase of the Ca^{2+} affinity of CaM upon complex formation with its targets (13).

Previous biochemical and structural studies of the EF-CaM interaction have provided insight into the activation of EF by CaM. Both the N- and C-terminal domains of CaM are essential for EF activity; however, only the Ca^{2+} binding ability of the C-terminal CaM domain is required for EF activity (14). The crystal structure of the $2Ca^{2+}$·CaM·EF complex shows that EF interacts with the closed N-terminal domain and the open C-terminal CaM domain in an extended conformation, with no direct contacts between the two domains (15). Activation of EF arises from the stabilization of a 12-residue-long catalytic loop, which is disordered in the CaM-free state.

The present study examines the interaction of EF with the three major Ca^{2+} states of CaM by NMR spectroscopy, with the aim to investigate whether and how the apo- and $4Ca^{2+}$-loaded

* This work was supported by National Institutes of Health Grants GM62548 and GM53459 (to W. J. T.). The costs of publication of this article were defrayed in part by the payment of page charges. This article must therefore be hereby marked "*advertisement*" in accordance with 18 U.S.C. Section 1734 solely to indicate this fact.

[S] The on-line version of this article (available at http://www.jbc.org) contains Supplemental Data.

§ Supported by a long term fellowship from the Human Frontier Science Program Organization.

** To whom correspondence may be addressed: NIH, Bldg. 37, Rm. 6106C, 37 Convent Dr., Bethesda, MD 20892-4255. Tel.: 301-496-3038; Fax: 301-402-3095; E-mail: ckl@helix.nih.gov.

‡‡To whom correspondence may be addressed: Ben-May Inst. for Cancer Research, JFK R120, 924 East 57th St., Chicago, IL 60637. Tel.: 773-702-4331; Fax: 773-702-3701; E-mail: tang@midway.uchicago.edu.

§§ To whom correspondence may be addressed: Laboratory of Chemical Physics, NIDDK, NIH, Bldg. 5, Rm. 126, 5 Center Dr., Bethesda, MD 20892-0520. Tel.: 301-496-2848; Fax: 301-402-0907; E-mail: bax@nih.gov.

[1] The abbreviations used are: EF, edema factor; CaM, calmodulin; HSQC, heteronuclear single-quantum coherence; TROSY, transverse relaxation optimized spectroscopy; HNCO, proton-nitrogen-carbonyl correlation; HNCA, proton-nitrogen-C^{α}.

forms of CaM interact with EF. Changes in Ca^{2+} affinities of CaM in the presence of EF are also assessed, using flow dialysis. We find that EF interacts weakly but specifically with the N-terminal domain of apoCaM, whereas the C-terminal CaM domain only engages in the interaction upon Ca^{2+} ligation. Interaction with EF strongly affects the Ca^{2+} affinity of CaM, with large increases for the C-terminal Ca^{2+} sites, and a strong decrease for sites in the N-terminal domain. Remarkably, NMR data indicate that CaM retains specific binding affinity for EF at all levels of Ca^{2+} ligation.

EXPERIMENTAL PROCEDURES

Protein Production and NMR Sample Preparation—Xenopus CaM, enriched with ^{13}C,^{15}N or ^{2}H,^{13}C,^{15}N, was produced as described previously (16). The expression and purification of anthrax EF (residues 291–800) followed previously published protocols (14). To strip the divalent cations away from EF, it was washed with a 50 mM EDTA, pH 8.0, 50 mM NaCl solution by three ultrafiltration-dilution cycles (1:10 dilution) and subsequently exchanged into a 50 mM NaCl solution, pH 7.0, by repeated ultrafiltration-dilution. CaM was treated analogously, but as CaM has a stronger affinity for Ca^{2+}, EDTA at pH 9.5 and 1:20 dilutions were used. Nevertheless, the final sample solution in the NMR tube typically contained 100 ± 10 μM Ca^{2+}, as measured by atomic absorption spectroscopy. Besides an EF-CaM sample with 0.3 mM CaM (ϵ_{280} = 3005 M^{-1} cm^{-1}) and 0.5 mM EF (Bradford assay), a CaM-only sample containing 0.2 mM of protein was also prepared to serve as a reference. Ca^{2+} was titrated into the sample solutions from a stock solution of 20 mM $CaCl_2$, 50 mM NaCl, pH 7.0. With a relatively low CaM concentration of 0.3 mM, the initial Ca^{2+} presence of 0.1 mM was found to have quite pronounced effects on the spectra. To acquire data below an effective Ca^{2+} concentration of 0.1 mM, the sample preparation was repeated, but this time EDTA was retained at 7.5 and 50 mM, and after additional buffer exchange, EDTA at 100 mM (without NaCl) was also used. An upper limit for the concentration of free Ca^{2+} in the presence of EDTA was estimated from the Ca^{2+} affinity of EDTA at pH 7.0 (17). For spectral assignment purposes, a third sample was also prepared, containing 0.5 mM CaM and 0.6 mM EF, in 5 mM $CaCl_2$, 50 mM NaCl, pH 7.0.

NMR Spectroscopy—Experiments were carried out on Bruker DRX800 and DRX600 spectrometers equipped with a room temperature probe and a cryogenic triple resonance probe, respectively. Data were processed with the NMRPipe package (18) and analyzed with NMRView (19). For each Ca^{2+} titration point, ^{1}H-^{15}N TROSY-HSQC spectra (20) were recorded at 800 MHz and 25 °C with acquisition times of 41 ms in the ^{1}H dimension and 51.2 ms in the ^{15}N dimension. Backbone H^N, C^α, C', and N chemical shifts for the Ca^{2+}-saturated state ($4Ca^{2+}$·CaM·EF) were obtained from TROSY-HNCO and TROSY-HNCA experiments (21), recorded at 600 MHz and 29 °C. For residues with characteristic H^N, C^α, C', and N chemical shifts, assignments were inferred by comparison with reported shifts in the apo- and Ca^{2+}-loaded CaM states. For a subset of these, sequential $^{13}C^{\alpha}_{i}$-$^{13}C^{\alpha}_{i-1}$ connectivities were available to confirm these assignments.

Flow Dialysis—Experiments were performed analogously to earlier descriptions (8, 22). In brief, the dialysis cell, comprising an upper and lower compartment built from Teflon, was thermostated at 25 °C. The upper chamber contained 6 μCi of $^{45}CaCl_2$ and 32 nmol of either CaM alone or of each CaM and EF in 2 ml 10 mM Hepes-KOH, pH 7.3, 100 mM KCl solution. CaM and EF were decalcified as described above; however, ensuing buffer exchange was performed by two gel filtration steps. Buffer exchange was complete as judged from the absence of ^{1}H EDTA NMR signals (data not shown). The Ca^{2+} concentrations of the buffer and sample solutions were determined by atomic absorption spectroscopy and calculated on the basis of the specific activity of $^{45}Ca^{2+}$. The lower dialysis cell chamber was perfused at a flow rate of 180 ml/h. Interval times between sample collections were 2.4–2.8 min. Six to seven fractions were collected after each addition of Ca^{2+} ligand, and 1 ml of each fraction was counted in 10 ml of Aquasol. Data were corrected for ligand depletion (11% of radioactivity added at the start of the experiment) and corrected for the low affinity Ca^{2+} binding to EF (23), which was determined independently. Macroscopic Ca^{2+}-CaM·EF dissociation constants, K, were determined by fitting the data to the Adair-Klotz equation (24) assuming four Ca^{2+}-binding sites,

$$N = \frac{x/K_1 + 2x^2/K_1K_2 + 3x^3/K_1K_2K_3 + 4x^4/K_1K_2K_3K_4}{1 + x/K_1 + x^2/K_1K_2 + x^3/K_1K_2K_3 + x_4/K_1K_2K_3K_4} \qquad \text{(Eq. 1)}$$

where N denotes the moles of bound Ca^{2+} per mole of CaM, x refers to the concentration of free Ca^{2+}, determined experimentally, and K_1, K_2, K_3, and K_4 are the fitted macroscopic dissociation constants.

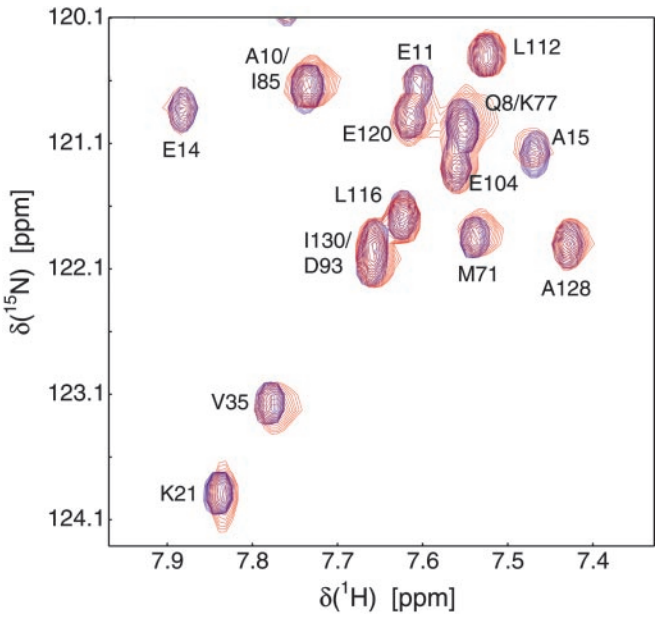

FIG. 1. **Superimposed regions of TROSY H-N correlation spectra of apoCaM in the presence and absence of EF.** The spectrum of free CaM is shown in *blue*, and the spectrum of apoCaM·EF is shown in *red*. Residues 1–75 and 83–148 constitute the N- and C-terminal domains of CaM, respectively. The spectra were recorded at 25 °C and 800 MHz in the presence of 100 mM EDTA, pH 7.0, with protein concentrations of 0.3 mM CaM and 0.5 mM EF. Under those conditions the fraction of apoCaM is estimated to be >99% of the total CaM.

RESULTS

In the course of a Ca^{2+} titration of CaM in the absence of EF, first the C-terminal and then the N-terminal CaM domain undergo well characterized structural and dynamic changes (5, 6). For example, NMR resonances whose chemical shift differ between the Ca^{2+}-free and bound states experience extensive broadening as a result of Ca^{2+} off-rates in the fast to intermediate exchange limit (25–27). When performing a Ca^{2+} titration of CaM in the presence of EF, spectral changes resulting from the Ca^{2+} dependence of the CaM-EF interaction superimpose on the effect of Ca^{2+} binding to CaM. This leads to relatively complex NMR spectra, but also gives some insights into the Ca^{2+} binding properties of CaM when bound to EF, in addition to the interaction of CaM with EF itself. By isotopically labeling only CaM, but not EF, the H-N backbone resonances of CaM, which are sensitive probes of the structural and dynamic environment of their associated residue, can be selectively examined. By NMR standards the CaM·EF complex of 76 kDa is quite large, but transverse relaxation optimized (TROSY) NMR experiments (28) made the study of this complex feasible.

The Interaction of Edema Factor with Apocalmodulin—In the presence of excess EF, the appearance of the H-N TROSY correlation spectrum of apoCaM is very similar to that of CaM in the absence of EF (Fig. 1). Only a small subset of resonances shift slightly in position and broaden severely, whereas the majority of resonances retain the same chemical shifts, while their ^{15}N line width increases by about 60%. If complex formation between apoCaM and EF would be complete, an increase in the ^{15}N line width by about a factor of five would be expected due to the slower tumbling of the 76-kDa complex compared with free CaM (16 kDa). The observed 60% increase in line width therefore indicates that only about 15% of CaM molecules are bound to EF, corresponding to a dissociation constant, K_D, of about 2 mM between apoCaM and EF.

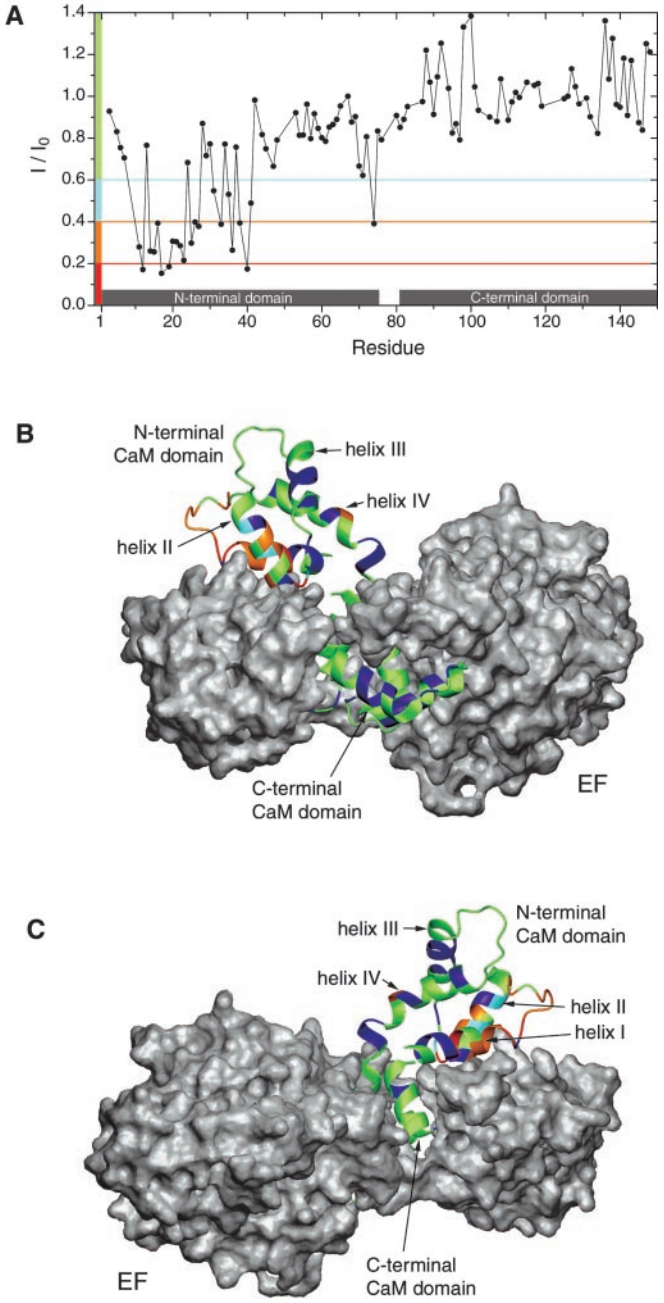

FIG. 2. **Interactions between apoCaM and EF.** *A*, ratios of the apoCaM resonance intensities in the absence, I_0, and presence of excess EF, I. The I/I_0 ratios were scaled to 1 for the largest N-terminal domain I/I_0 value (obtained for Glu^{67}). Error bars resulting from spectral noise are small (<1%) and have been omitted for clarity. Gaps arise from spectral overlap. Residues 1–75 and 83–148 constitute the N- and C-terminal domains of CaM, respectively, which are connected by a seven-residue linker. *B* and *C*, I/I_0 ratios color-coded on the crystal structure of CaM in the $2Ca^{2+}$·CaM·EF complex. The color-coding of the CaM ribbon representation is depicted in *A*. Residues for which no information could be obtained are colored blue. The van der Waals surface of EF is shown in *gray*. *B* and *C* are related by a 180° rotation about the vertical axis.

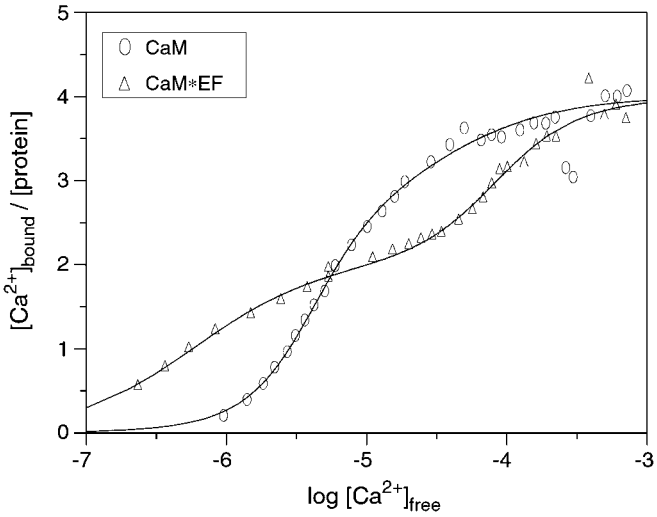

FIG. 3. **Ca^{2+}-binding curves of free CaM and CaM·EF.** The number of bound Ca^{2+} per CaM as a function of free Ca^{2+} concentration was obtained by flow dialysis. Fits of the data to the Adair-Klotz equation (Equation 1) are shown. The obtained apparent dissociation constants are given in Table I.

TABLE 1
Apparent macroscopic dissociation constants, K, for the four Ca^{2+} binding sites in free CaM and the CaM-EF complex

Values are derived from the data shown in Fig. 3 recorded in 10 mM Hepes-KOH, pH 7.3, 100 mM KCl. The residual S.D. in the global fit was 0.11 for CaM·EF and 0.08 for free CaM.

	K_1	K_2	K_3	K_4
	μM	μM	μM	μM
CaM·EF	0.3	1.1	106	67
CaM	5.6	2.7	6.5	48

A comparison of the broadening of individual resonances, expressed most conveniently as ratios between the signal intensity of free CaM, I_0, and CaM in the presence of EF, I, shows that all strongly broadened resonances belong exclusively to the N-terminal CaM domain (Fig. 2*A*). In the millimolar affinity range of the interaction between apoCaM and EF, the selective broadening of a subset of resonances is generally caused by exchange kinetics between free and EF-bound CaM that is fast on the NMR chemical shift timescale ($>10^4$ s^{-1}). This broadening is then proportional to the square of the chemical shift difference (expressed in frequency units) between the free and bound state. A low signal intensity ratio between the H-N correlations in the presence and absence of EF, I/I_0, therefore correlates with the magnitude of the EF-induced structural perturbation experienced by the H^N and ^{15}N nuclei of a particular CaM residue. The obtained intensity ratios, color-coded on the crystal structure of $2Ca^{2+}$·CaM·EF, show good agreement with the N-terminal domain-EF contacts, observed in this structure (Fig. 2, *B* and *C*). This indicates that apoCaM binds EF through its N-terminal domain in a manner that parallels the interaction observed in the crystal structure of $2Ca^{2+}$·CaM·EF, whereas the closed C-terminal domain does not make specific contacts with EF.

Ca^{2+} Affinities of Calmodulin in the Presence of Edema Factor—To separate the effects of Ca^{2+} binding from those of the CaM-EF interaction, we resorted to flow dialysis experiments, which yield a direct measure for the effect of EF on the Ca^{2+} affinity of CaM. The Ca^{2+} titration curve (Fig. 3) reveals an approximately 20-fold increase in affinity for the binding of the first Ca^{2+} ion in the presence of EF (Table I), but binding of the second Ca^{2+}, which occurs with an ~2-fold increased affinity, is no longer cooperative (Hill coefficient of ~1). A likely explanation for this finding is seen in the crystal structure of the $2Ca^{2+}$·CaM·EF complex; the distance from Ca^{2+} at calcium binding site 3 to the carboxyl group of Asp^{93} of CaM in the EF-CaM complex is 3.1 Å, which is 0.9 Å longer than in free CaM, and is clearly quite unfavorable. This therefore assigns the highest Ca^{2+} affinity of CaM in the presence of EF to site 4, comprising residues Asn^{129}–Glu^{140}. Interestingly, the Ca^{2+} affinities of the N-terminal domain binding sites are significantly

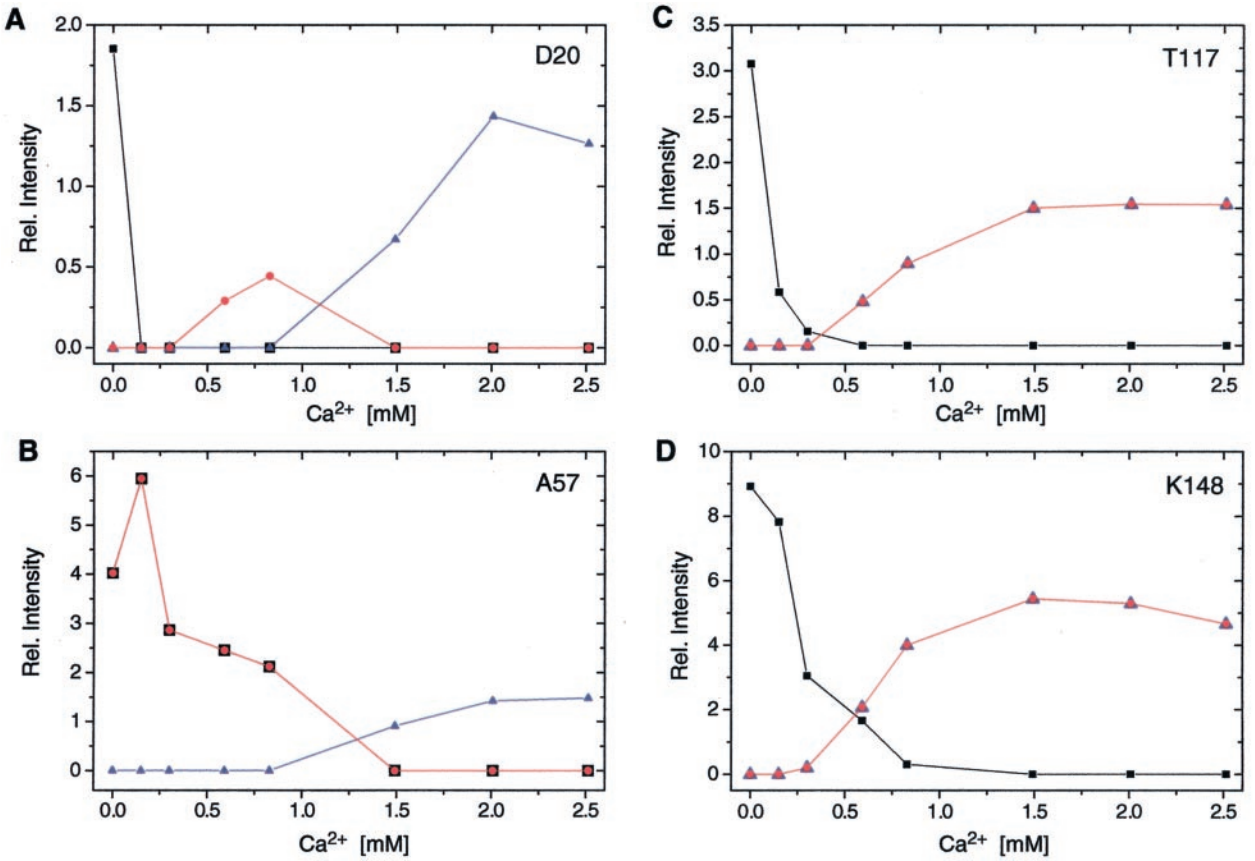

FIG. 4. **Ca^{2+} titration of CaM in the presence of EF.** The H-N TROSY signal intensities of residues Asp^{20} (*A*), Ala^{57} (*B*), Thr^{117} (*C*), and Lys^{148} (*D*) quantified at spectral positions corresponding to apoCaM·EF (■), $2Ca^{2+}$·CaM·EF (*red circles*), and $4Ca^{2+}$·CaM·EF (*blue triangles*). A signal intensity of 0 denotes that no resonance above the noise threshold could be detected at the position in question. The initial protein concentrations were 0.3 mM CaM and 0.5 mM EF. The signal intensities were corrected for the sample dilutions incurred upon Ca^{2+} addition.

reduced compared with free CaM (Fig. 3 and Table I), consistent with the observation that no calcium ions were observed in the N-terminal domain of CaM in the structure of EF-CaM complex (15).

Calmodulin-Edema Factor Interactions in the Two Ca^{2+} CaM State—Large changes in the NMR spectrum of CaM in the presence of EF are observed upon addition of Ca^{2+}. These changes are illustrated by the behavior of four resonances, comprising two C-terminal domain residues (Thr^{117} and Lys^{148}) and two N-terminal domain residues (Asp^{20} and Ala^{57}). For these residues spectral assignment could be maintained throughout the entire Ca^{2+} titration. In the current section, the effects of going from CaM·EF to $2Ca^{2+}$·CaM·EF are discussed, *i.e.* up to the point where Ca^{2+} loading of the C-terminal domain of CaM calcium-binding sites is nearly complete, while the calcium binding sites of the CaM N-terminal domain are predominately in the apo state.

Ala^{57} of the N-terminal domain makes no direct contact with EF (Fig. 2*A*), but its H-N resonance becomes increasingly broadened upon Ca^{2+} binding by the C-terminal domain (Fig. 4*B*). In the titration of the C-terminal CaM domain, the chemical shift of Ala^{57} remains essentially unaltered, *i.e.* δ(apoCaM·EF) = $\delta(2Ca^{2+}$·CaM·EF), indicating that its resonance broadening is caused by increasingly slower averaged tumbling rates that result from an increase in EF-CaM complex formation. The resonance of Asp^{20}, which is in direct contact with EF and which was severely broadened in the apoCaM state, reappears with higher intensity (Fig. 4*A*). The exchange broadening of Asp^{20} has vanished, reflecting a change in CaM-EF exchange kinetics from fast for apoCaM to slow for $2Ca^{2+}$·CaM. This indicates a much reduced off-rate ($<100\ s^{-1}$) for $2Ca^{2+}$·CaM binding to EF compared with apoCaM. Slow exchange kinetics are also evidenced by the simultaneous presence of both the EF-bound and EF-free resonance of the C-terminal residue, Lys^{148}, during the titration of the C-terminal CaM domain (Fig. 4*D*). Lys^{148} is one of the few C-terminal domain residues whose H-N chemical shifts are not affected by Ca^{2+} binding and therefore monitors exclusively the CaM-EF interaction. In contrast, the vast majority of C-terminal residues, such as Thr^{117}, experience a Ca^{2+}-dependent exchange process that broadens them beyond detection at intermediate Ca^{2+} levels (Fig. 4*C*). Only after Ca^{2+} complex formation progresses toward completion, the resonances reappear at positions that differ from free $2Ca^{2+}$·CaM by an additional chemical shift, $\Delta\delta_{EF}$, resulting from the new EF-bound environment. For the N-terminal domain residues of CaM that interact with EF (Fig. 2*A*), the apoCaM·EF peak positions are displaced toward the $2Ca^{2+}$·CaM·EF resonances by about 10–15% relative to free CaM (data not shown). This agrees well with the estimated 15% fraction of apoCaM·EF complex formation obtained above from the line width increase.

Calmodulin-Edema Factor Interactions in the Saturated, Four Ca^{2+} CaM State—When continuing the Ca^{2+} titration, Ca^{2+}-induced exchange broadening of the N-terminal domain residues is observed, *e.g.* Asp^{20} and Ala^{57} (Fig. 4, *A* and *B*). For the C-terminal domain residues, a slight increase in signal intensities is observed (*e.g.* Thr^{117} and Lys^{148}; Fig. 4, *C* and *D*), resulting from the completion of Ca^{2+} saturation of the C-terminal domain binding site 3. Analogous to what was observed above for the N-terminal domain residues upon Ca^{2+} binding of the C-terminal domain, the chemical shift of the C-terminal domain residues remain essentially unchanged

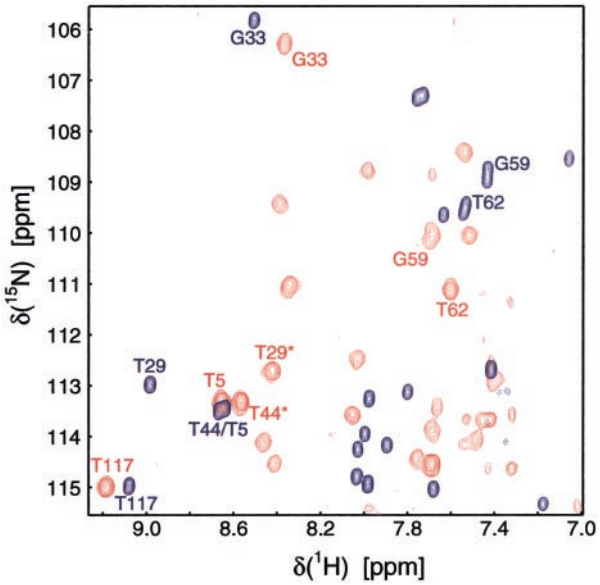

FIG. 5. **Superimposed regions of TROSY H-N correlation spectra of Ca^{2+}-saturated CaM in the presence and absence of EF.** The spectrum of $4Ca^{2+}$·CaM is shown in *blue*, and the spectrum of $4Ca^{2+}$·CaM·EF is shown in *red*. Both spectra were recorded at 25 °C and 800 MHz in the presence of 4 mM Ca^{2+} at pH 7.0, with protein concentrations of about 0.3 mM CaM and 0.5 mM EF. The $4Ca^{2+}$·CaM chemical shifts in the presence of EF differ from free $4Ca^{2+}$·CaM. CaM resonances of $4Ca^{2+}$·CaM·EF for which assignments could be obtained are labeled together with their corresponding $4Ca^{2+}$·CaM resonances. Tentative assignments, based on comparison of characteristic ^1H, ^{15}N, and $^{13}C'$ chemical shifts, and for which sequential connectivities were below the noise threshold, are indicated by an *asterisk*.

upon Ca^{2+} ligation of the N-terminal domain, *i.e.* $\delta(2Ca^{2+}\cdot CaM\cdot EF) = \delta(4Ca^{2+}\cdot CaM\cdot EF)$ (data not shown; *cf.* also Fig. 4, *C* and *D*). In contrast, the N-terminal domain residues undergo substantial chemical shift changes, $\Delta\delta_{Ca^{2+}}$, in addition to the changes, $\Delta\delta_{EF}$, seen upon binding of apoCaM to EF. Moreover, comparison of the $4Ca^{2+}$·CaM·EF chemical shifts with those of $4Ca^{2+}$·CaM indicates that the $\Delta\delta_{EF}$ shift change is not reversed by Ca^{2+} binding (Fig. 5). Thus, the N-terminal CaM domain remains able to bind Ca^{2+} and does not dissociate from EF upon Ca^{2+} binding.

As the N-terminal CaM domain initially binds to EF in the closed conformation, the question arises whether Ca^{2+} binding leads to the "opening" of this domain. In the open state, CaM helices I and II are oriented nearly perpendicular to one another, but opening of the I/II interhelical angle is hindered by the interactions both helices make with EF (Fig. 2, *B* and *C*). Helices III and IV do not directly contact EF, but they make hydrophobic contacts with I and II. Unlike for the C-terminal CaM domain, where EF selectively binds the open domain state, resulting in increased Ca^{2+} affinity, the considerably decreased Ca^{2+} affinity of the N-terminal domain suggests that EF favors binding the closed N-terminal domain state. The marked differences in H-N chemical shifts between $4Ca^{2+}$·CaM·EF and $4Ca^{2+}$·CaM for N-terminal domain residues that are not in direct contact with EF (*e.g.* Ala^{57}, Gly^{59}, and Thr^{62}; Fig. 5) indicate that the structure for the N-terminal Ca^{2+}-ligated domain differs from the open conformation in $4Ca^{2+}$·CaM. However, whether an intermediate degree of opening takes place cannot be assessed by the data at hand. In principle, a chemical shift comparison between $4Ca^{2+}$·CaM·EF and $4Ca^{2+}$·CaM could highlight all sites affected by either EF or the difference in structure, analogous to Fig. 2. Unfortunately, the high molecular weight of the complex (76 kDa) in combination with weak aggregation above about 0.3 mM CaM, as indicated by ^{15}N relaxation data, did not permit the assignment of a sufficiently large number of resonances in the $4Ca^{2+}$·CaM·EF state to make such an analysis. In this respect, it is also interesting to note that despite an excess of Ca^{2+} during crystal growth, only the $2Ca^{2+}$·CaM·EF state is observed, with relatively high crystallographic *B*-factors for the N-terminal domain (15). These high temperature factors are indicative of some structural heterogeneity, possibly arising from the presence of a small amount of $4Ca^{2+}$·CaM·EF.

DISCUSSION

By comparing CaM ^1H-^{15}N NMR resonance intensities in the presence and absence of EF, our data indicate that EF binds the N-terminal domain of apoCaM in a manner that parallels the interaction observed in the crystal structure of $2Ca^{2+}$·CaM·EF, *i.e.* when the Ca^{2+}-bound C-terminal domain is also interacting with EF. The closed C-terminal CaM domain does not participate significantly in the apoCaM·EF interaction, which is estimated to take place with a K_D of about 2 mM. With the calcium-free C-terminal CaM domain not binding to EF, we speculate it may sterically interfere with optimal N-terminal CaM domain interaction with EF. Only little catalytic activity of EF at 50 nM or lower Ca^{2+} concentrations has been reported (23). This agrees well with the picture that EF activation is induced by conformational changes arising mainly from interactions between EF and the C-terminal domain of CaM (15), and our observation that the C-terminal domain does not interact with EF in the closed, apo form.

Upon titrating Ca^{2+} into the CaM and EF containing sample, the C-terminal domain engages in the interaction with EF without affecting the N-terminal domain-EF interactions. A detailed picture of this state is provided by the recently reported crystal structure (15). EF binding to the open C-terminal domain also leads to the stabilization of this structural state as evidenced by approximately 20- and 2-fold increased Ca^{2+} affinities for the first and second Ca^{2+}-binding sites, respectively, compared with free CaM. Ca^{2+} binding to the N-terminal CaM domain proceeds with considerably reduced affinities compared with free CaM, suggesting that EF opposes opening of this domain, which is perhaps not surprising given its well defined contacts with the closed domain. The extent of any N-terminal CaM domain opening upon Ca^{2+} ligation in the complex poses an interesting question, which could not be answered with the data at hand. However, differences in chemical shifts between the free and EF-bound states indicate that the N-terminal domain maintains contact with EF. Clearly, N-terminal domain Ca^{2+} ligation is negligible at physiological Ca^{2+} levels and is not needed for enzymatic activity. This agrees with the findings that mutational inactivation of the N-terminal Ca^{2+}-binding site of CaM has no effect on EF activity (14) and that the CaM mutant N41C,K75C, locked in the closed conformation by the Cys^{41}-Cys^{75} disulfide bond, exhibits the same Ca^{2+} dependence of EF activation as does wild-type CaM (23).

Taking together our NMR analysis and the crystal structures of EF alone and in complex with CaM, we propose the model for the EF-CaM interaction depicted in Fig. 6. In this model, EF exists in two structural states: a closed state, termed EF^c, represented by the structure of EF alone, and an open state, termed EF^o, represented by the structure of EF in the $2Ca^{2+}$·CaM·EF complex. In the EF^c state, the catalytic core (C_A and C_B) and helical domains (Fig. 6), which together constitute the adenylyl cyclase domain, form an extensive contact surface of about 3600 Å^2. Binding of the C-terminal CaM domain disrupts this contact surface, in contrast to the binding of the N-terminal CaM domain, which takes place at a largely solvent-exposed site of the helical domain. N-terminal domain interactions with EF are therefore an efficient point of initial contact between the two proteins. The binding of N-terminal

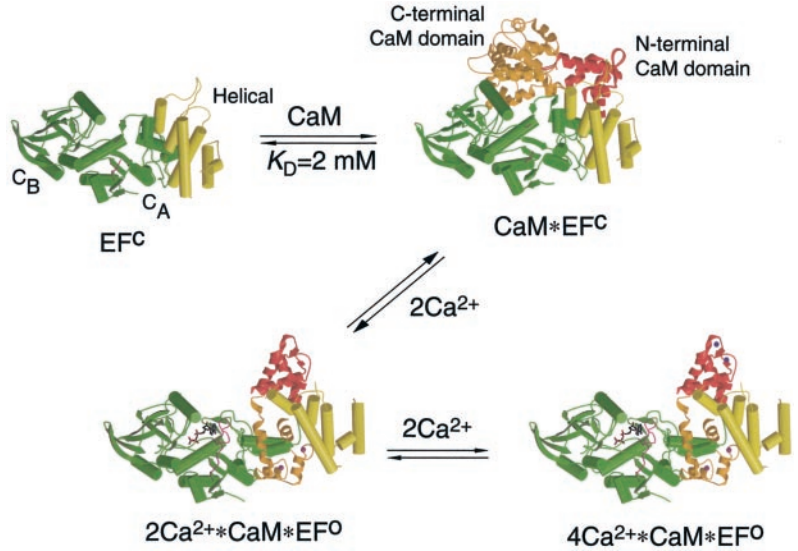

FIG. 6. **Model of the EF-CaM interaction.** EF^c and EF^o denote closed and open states of EF, represented by the structure of EF alone (Protein Data Bank accession code 1K8T), and in complex with 2Ca^{2+}·CaM (Protein Data Bank accession code 1K90), respectively. The catalytic core (domains C_A and C_B) is shown in *green*, the helical domain in *yellow*, the catalytic loop in *magenta*, and ATP in *black*. CaM·EF^c is represented by the superposition of the N-terminal CaM domain of three structures from the bundle of apoCaM NMR structures (Protein Data Bank accession code 1CFC) onto the helical domain of EF^c based on the N-terminal CaM domain-EF contacts in the 2Ca^{2+}·CaM·EF crystal structure. The N-terminal CaM domain is shown in *red*, the C-terminal CaM domain in *brown*, and calcium ions in *purple*. Only the average of the 20% fraction of the bundle of apoCaM NMR structures that permits superposition without causing steric clashes with EF^c is shown. 4Ca^{2+}·CaM·EF is depicted here with the N-terminal CaM domain still in the closed state. The extent of N-terminal domain opening could not be determined from the data at hand (see "Discussion").

CaM to the EF helical domain places the C-terminal CaM against the interface of C_A and C_B. Conceivably, the restricted flexibility of the linker between the N- and C-terminal domains of apoCaM will then facilitate crossing of the energy barrier associated with the dissociation between the catalytic core and helical domains. The extensive interaction surface of about 6000 Å^2 between the C-terminal CaM domain and both catalytic core and helical domains will then make up the enthalpic loss from the contact between catalytic core and helical domains. Such a model is consistent with the recent observation that a mixture of the isolated N- and C-terminal CaM domains cannot reconstitute the EF catalytic activity observed for CaM (23).

In the presence of EF, our study reveals significantly enhanced Ca^{2+} affinities of the two C-terminal Ca^{2+}-binding sites of calmodulin, accompanied by a loss in their cooperativity. The N-terminal CaM domain experiences a large reduction of Ca^{2+} affinities, but gains in cooperativity. However, as Ca^{2+} binding to the N-terminal domain is not relevant for EF activation, unlike for most other cellular targets of CaM (12), EF appears to be significantly activated before maximum activation is reached for most endogenous cellular CaM targets. Even at free Ca^{2+} concentrations found in resting cells of 0.05–0.1 μM, *in vitro* experiments have shown that EF is already significantly activated, but, as observed *in vivo* as well as *in vitro*, elevated Ca^{2+} levels are required for full activation, although eventually a decrease in EF activity is observed (23, 29). This behavior differs significantly from the related adenylyl cyclase toxin CyaA from *Bordetella pertussis*, which appears to bind CaM in a Ca^{2+}-independent manner and is highly active even at resting cellular Ca^{2+} concentrations (23).

Acknowledgment—We thank James Chou for useful discussions.

REFERENCES

1. Leppla, S. H. (1982) *Proc. Natl. Acad. Sci. U. S. A.* **79,** 3162–3166
2. Mourez, M., Lacy, D. B., Cunningham, K., Legmann, R., Sellman, B. R., Mogridge, J., and Collier, R. J. (2002) *Trends Microbiol.* **10,** 287–293
3. Pannifer, A. D., Wong, T. Y., Schwarzenbacher, R., Renatus, M., Petosa, C., Bienkowska, J., Lacy, D. B., Collier, R. J., Park, S., Leppla, S. H., Hanna, P., and Liddington, R. C. (2001) *Nature* **414,** 229–233
4. Bradley, K. A., Mogridge, J., Mourez, M., Collier, R. J., and Young, J. A. T. (2001) *Nature* **414,** 225–229
5. Ikura, M. (1996) *Trends Biochem. Sci.* **21,** 14–17
6. Nelson, M. R., and Chazin, W. J. (1998) *Biometals* **11,** 297–318
7. Crivici, A., and Ikura, M. (1995) *Annu. Rev. Biophys. Biomol. Struct.* **24,** 85–116
8. Haiech, J., Klee, C. B., and Demaille, J. G. (1981) *Biochemistry* **20,** 3890–3894
9. Linse, S., Helmersson, A., and Forsen, S. (1991) *J. Biol. Chem.* **266,** 8050–8054
10. Tsien, R. Y., Pozzan, T., and Rink, T. J. (1984) *Trends Biochem. Sci.* **9,** 263–266
11. Tsien, R. Y., Pozzan, T., and Rink, T. J. (1982) *J. Cell Biol.* **94,** 325–334
12. Hoeflich, K. P., and Ikura, M. (2002) *Cell* **108,** 739–742
13. Huang, C. Y., Chau, V., Chock, P. B., Wang, J. H., and Sharma, R. K. (1981) **78,** 871–874
14. Drum, C. L., Yan, S. Z., Sarac, R., Mabuchi, Y., Beckingham, K., Bohm, A., Grabarek, Z., and Tang, W. J. (2000) *J. Biol. Chem.* **275,** 36334–36340
15. Drum, C. L., Yan, S. Z., Bard, J., Shen, Y. Q., Lu, D., Soelalman, S., Grabarek, Z., Bohm, A., and Tang, W. J. (2002) *Nature* **415,** 396–402
16. Ikura, M., Marion, D., Kay, L. E., Shih, H., Krinks, M., Klee, C. B., and Bax, A. (1990) *Biochem. Pharmacol.* **40,** 153–160
17. Martell, A. E., and Smith, R. M. (1977) *Critical Stability Constants*, Plenum Press, New York
18. Delaglio, F., Grzesiek, S., Vuister, G. W., Zhu, G., Pfeifer, J., and Bax, A. (1995) *J. Biomol. NMR* **6,** 277–293
19. Johnson, B. A., and Blevins, R. A. (1994) *J. Biomol. NMR* **4,** 603–614
20. Pervushin, K. V., Wider, G., and Wuthrich, K. (1998) *J. Biomol. NMR* **12,** 345–348
21. Salzmann, M., Pervushin, K., Wider, G., Senn, H., and Wuthrich, K. (1998) *Proc. Natl. Acad. Sci. U. S. A.* **95,** 13585–13590
22. Stemmer, P. M., and Klee, C. B. (1994) *Biochemistry* **33,** 6859–6866
23. Shen, Y., Lee, Y. S., Soelaiman, S., Bergson, P., Lu, D., Chen, A., Beckingham, K., Grabarek, Z., Mrksich, M., and Tang, W. J. (2002) *EMBO J.* **21,** 6721–6732
24. Edsall, J. T., and Wyman, J. (1958) *Biophysical Chemistry*, Vol. 1, pp. 591–662, Academic Press, New York
25. Malmendal, A., Evenas, J., Forsen, S., and Akke, M. (1999) *J. Mol. Biol.* **293,** 883–899
26. Evenas, J., Malmendal, A., Thulin, E., Carlstrom, G., and Forsen, S. (1998) *Biochemistry* **37,** 13744–13754
27. Ikura, M., Hiraoki, T., Hikichi, K., Minowa, O., Yamaguchi, H., Yazawa, M., and Yagi, K. (1984) *Biochemistry* **23,** 3124–3128
28. Riek, R., Pervushin, K., and Wuthrich, K. (2000) *Trends Biochem. Sci.* **25,** 462–468
29. Kumar, P., Ahuja, N., and Bhatnagar, R. (2002) *Infect. Immun.* **70,** 4997–5007